

SHORT COMMUNICATION



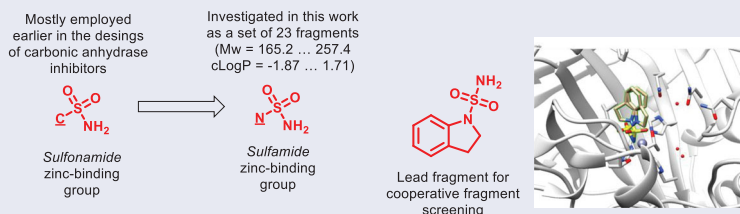
Diversely substituted sulfamides for fragment-based drug discovery of carbonic anhydrase inhibitors: synthesis and inhibitory profile

Tatiana Sharonova^a, Petr Zhmurov^a, Stanislav Kalinin^a, Alessio Nocentini^b , Andrea Angeli^b , Marta Ferraroni^b, Mikhail Korsakov^c, Claudiu T. Supuran^b  and Mikhail Krasavin^a

^aInstitute of Chemistry, Saint Petersburg State University, Saint Petersburg, Russia; ^bNeurofarba Department, Università Degli Studi di Firenze, Florence, Italy; ^cPharmaceutical Technology Transfer Center, Ushinsky Yaroslavl State Pedagogical University, Yaroslavl, Russia

ABSTRACT

A series of sulfamide fragments has been synthesised and investigated for human carbonic anhydrase inhibition. One of the fragments showing greater selectivity for cancer-related isoforms *hCA IX* and *XII* was co-crystallized with *hCA II* showing significant potential for fragment periphery evolution *via* fragment growth and linking. These opportunities will be identified in the future *via* the screening of this fragment structure for co-operative carbonic anhydrase binding with other structurally diverse fragments.



ARTICLE HISTORY

Received 21 February 2022
Accepted 3 March 2022

KEYWORDS

Carbonic anhydrase; zinc-binding groups; sulfamides; co-operative fragment screening; solubility

1. Introduction

The carbonic anhydrase (CA) family of Zn(II) metalloenzymes (EC 4.2.1.1) catalyses the reversible hydration of carbon dioxide to bicarbonate anion, a fundamental reaction that controls physiological processes requiring pH control as well as ion transport and fluid secretion¹. Hyperactivity of specific CA isoforms² in various disease states makes these enzymes potential (and sometimes already validated) targets for therapeutic intervention with small molecule carbonic anhydrase inhibitors (CAIs)³.

Clinically validated applications of CAIs currently include, among other diseases, the treatment of glaucoma⁴, idiopathic intracranial hypertension⁵, high-altitude sickness⁶, congestive heart failure⁷, peptic ulcers⁸ and epilepsy⁹. Another important potential application of CAIs (specifically, of related human (*h*) CA IX and XII isoforms¹⁰) is in neoplastic therapy¹¹. The current state of development in this field is underscored by the *hCA IX*-selective drug SLC-0111¹² which is undergoing phase 1b clinical study for tumours overexpressing *hCA IX*¹³ and non-selective inhibitor E7070 (indisulam) developed by Eisai Co., Ltd. which successfully completed phase II clinical study¹⁴. The highly promising application of CAIs as antibacterials is based on the premise of selective inhibition of microbial CAs (crucial for the survival of bacteria) without affecting the CAs in the same concentration range¹⁵. Thus, CA inhibition from such microorganisms as *Vibrio cholerae*¹⁶, *Burkholderia pseudomallei*¹⁷, *Mycobacterium tuberculosis*¹⁸,


*Salmonella enterica*¹⁹, *Helicobacter pylori*²⁰, *Escherichia coli*²¹ and many others¹⁵.

Considering the plethora of validated and potential therapeutic applications of CAIs, the discovery of new chemotypes endowed with CA inhibitory activity will continue to be a significant aim. CA contains a Zn²⁺ ion in its active site which mandates the zinc-binding nature of active site targeting pharmacophoric groups which can be employed in the design of new CAIs. Indeed, most of the clinically investigated (SLC-0111 and E7070) and used (e.g. acetazolamide, methazolamide, dorzolamide, brinzolamide and zonisamide) are primary sulphonamides (CSO₂NH₂) in which the sulphonamide group anchors to the prosthetic zinc ion and the molecular periphery defines the potency and isoform selectivity of these CAIs² (Figure 1).

Many other zinc-binding motifs have been implicated as warheads in the CAI design²². Among them, sulfamides (NSO₂NH₂) appears as an attractive alternative to the frequently studied sulphonamides. Indeed, sulphonamides are expected to have greater polarity and solubility compared to sulphonamides, due to the presence of an additional nitrogen atom. Moreover, primary sulphonamide group is found in such drugs as anticancer epacadostat²³ and gastric ulcer medication famotidine²⁴, both of which (epacadostat²⁵ and famotidine²⁶) were also found to inhibit various CA isoforms (Figure 2).

The discovery of novel sulfamide CAIs would traditionally entail synthesis of structurally diverse libraries of compounds and their

CONTACT Claudiu T. Supuran  claudiu.supuran@unifi.it  Neurofarba Department, Università Degli Studi di Firenze, Florence, 50121 Italy; Mikhail Krasavin  mkrasavin@hotmail.com, krasavintm@gmail.com  Institute of Chemistry, Saint Petersburg State University, Saint Petersburg, Russia

 Supplemental data for this article can be accessed [here](#).

© 2022 The Author(s). Published by Informa UK Limited, trading as Taylor & Francis Group.

This is an Open Access article distributed under the terms of the Creative Commons Attribution License (<http://creativecommons.org/licenses/by/4.0/>), which permits unrestricted use, distribution, and reproduction in any medium, provided the original work is properly cited.

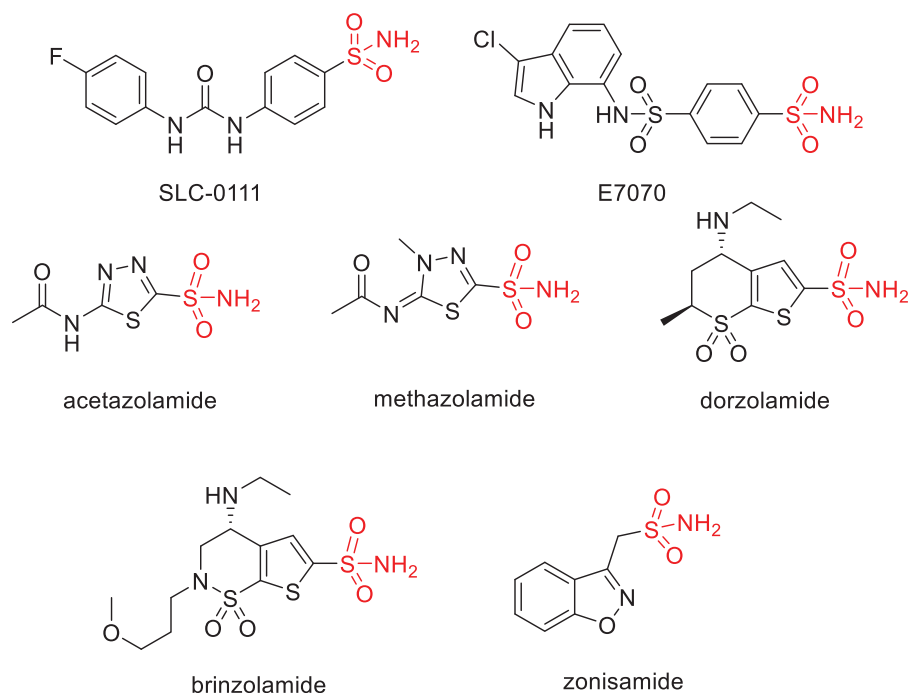


Figure 1. CAIs in clinical development and clinical use.

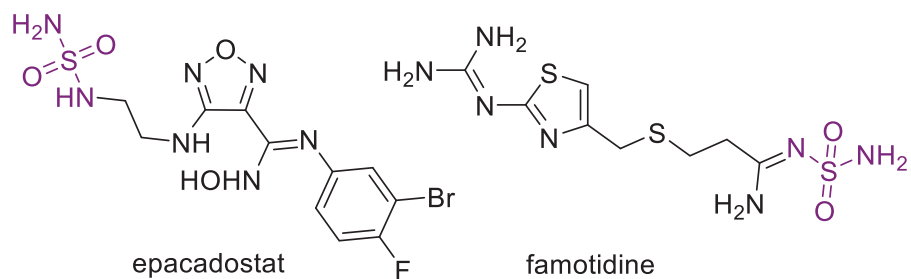


Figure 2. Examples of clinically used sulfamide drugs.

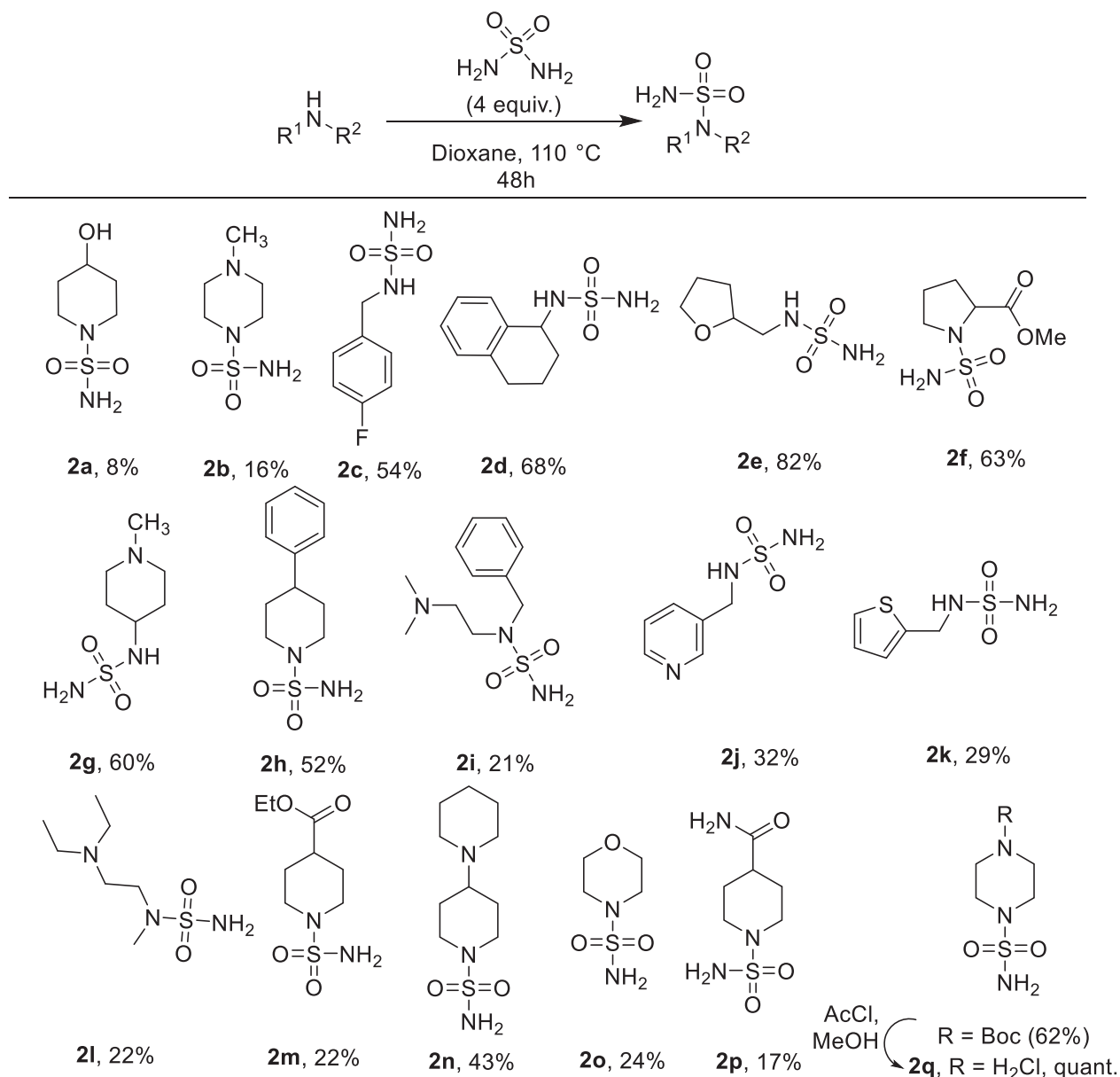
screening against an isoform panel of CAs. We have recently validated an approach²⁷ to the discovery of new sulphonamide CAIs based on the simultaneous screening of a diverse set of chemical fragments (i.e. small, Mw <~250 and polar, cLopP < 3.0²⁸) along with sulphonamide zinc-binding warhead (in particular, benzene-sulfonamide or BSA). This led not only to the discovery of over 100 fragment hits which potentiated the binding of BSA but also to rediscovery of BSA-based CAIs with the molecular periphery replicating the fragment co-binders. In our intent aimed at the discovery of novel sulfamide CAIs, we decided to take a similar approach. Realisation of such an approach would require synthesis of a library of fragment-like sulfamides and profiling them against a panel of human CAs (in this case, anti-glaucoma target *hCA* II, two membrane-associated cancer-related targets *hCA* IX and XII and the usual cytosolic off-target *hCA* I). In this work, we aimed at the realisation of this approach and selection of a suitable sulfamide zinc-binding warhead for fragment-based discovery of novel sulfamide-type CAIs, a chemotype much less studied in the context of CA inhibition compared to sulphonamides²⁹. Moreover, in this study, we were looking to identify: fragments that do not display apparently high intrinsic selectivity towards specific CA isoforms (mindful that such a selectivity will be gained in the future from co-operative screening of specific “tail” fragments³⁰) and yet would show a tendency to inhibit cancer-related isoforms *hCA* IX and XII over cytosolic *hCA* I and II. Of particular interest would be fragments that do not display a pronounced potency against CA

isoforms of interest, ideally in the 10⁻⁷M range of K_i values (so that the future contribution from co-operative fragment binding would be more pronounced). Specific emphasis was put on conformationally constrained fragments which would be structurally close to the classical BSA zinc-binding motif and would co-crystallize with any of the isoforms (e.g. the most readily available *hCA* II) to further guide further fragment evolution *via* growing, linking and merging³¹. Herein, we report on the successful realisation of this strategy.

2. Results and discussion

Seventeen non-symmetrically substituted primary sulfamides were synthesised from inorganic sulfamide **1** *via* direct nucleophilic substitution at the sulphur atom, *via* the thermally promoted reaction in dioxane with a four-fold excess of **1**, conducted at 110 °C over 48 h³². The yields of the resulting compounds **2a–q** were generally modest to good (Scheme 1).

The same thermally promoted protocol, not unexpectedly, did not work for less reactive (hetero)aromatic amines. Thus, an alternative approach was taken³³. Instead of sulfamide, commercially available chlorosulfonyl isocyanate **3** dissolved in dichloromethane at 0 °C was reacted with 1 equiv of *tert*-butanol to give the Boc-protected amino-sulfonyl-chloride (**4**), which was subsequently added slowly to a solution of 1 equiv of the respective



Scheme 1. Synthesis of unsymmetrically substituted primary sulfamides **2a–q**.

hetero(aromatic) amine in the presence of 2 equiv of triethylamine in dichloromethane at 0 °C. In this case, again, the yields of unsymmetrically substituted primary sulfamides **2r–w** were modest to good over two steps (Scheme 2).

From the physicochemical data summarised for fragments **2a–w** in Table 1, one can appreciate their being distinctly fragment-like ($M_w = 165.2 \dots 257.4$, $\text{cLogP} = -1.87 \dots 1.71$). Furthermore, the inhibitory data reveal the absence of apparent isoform selectivity displayed by these fragments which is perfectly in line with the limited size of the molecular periphery (typically responsible for making additional contacts with the protein and ensuring higher potency and isoform selectivity). With our initial focus on the cancer-related, membrane-bound CA isoforms *hCA IX* and *XII* compounds displaying greater selectivity towards these isoforms against cytosolic *hCA I* and *II* (structural homologs of each other **2r** and **2v**) received our priority attention.

After much experimentation, compound **2v** was co-crystallized with recombinant *hCA II* and its structure was resolved (Figure 3).

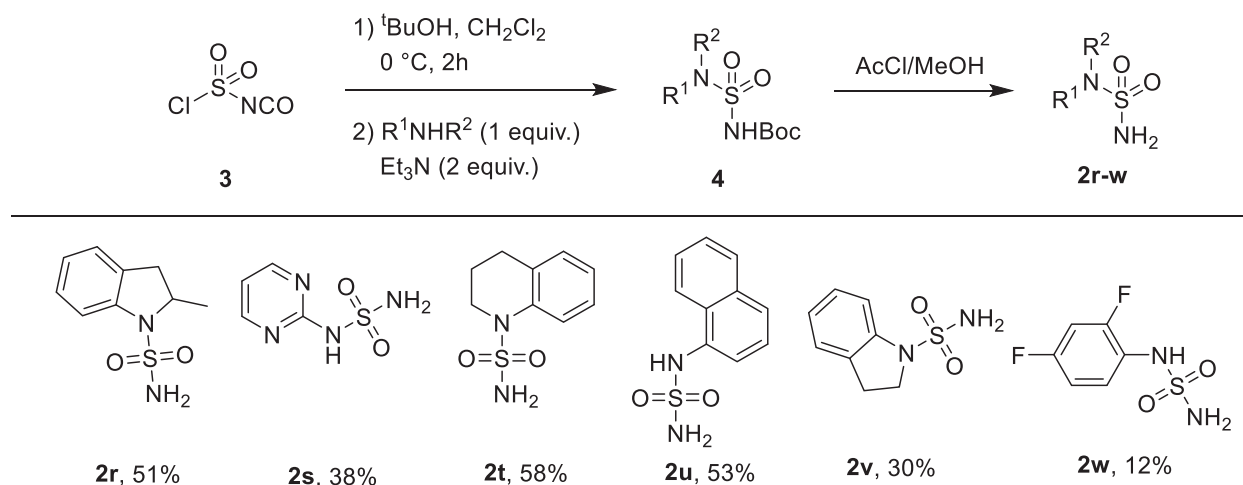
As one can see from the crystal structure of **2v** with *hCA II* isoform, the small ($M_w = 198.2$) *N*-(aminosulfonyl)indoline fragment

displayed two finding poses within the *hCA II* active site. In both poses, the sulfonamino groups are anchored to the prosthetic zinc ion (displayed as a grey sphere). The validity of the two binding poses signifies the fact that the binding of **2v** leaves a significant room for the periphery growth around this fragment and makes it a highly suitable candidate for co-operative screening with other structurally diverse fragments in order to identify the starting points for the structural evolution of this fragment.

3. Materials and methods

3.1. Chemical synthesis – general

NMR spectra were recorded on a Bruker Avance III 400 spectrometer (^1H : 400.13 MHz; ^{13}C : 100.61 MHz; chemical shifts are reported as parts per million (δ , ppm); the residual solvent peaks were used as internal standards: δ 7.28 ^1H in CDCl_3 , δ 77.02 ppm for ^{13}C in CDCl_3 ; multiplicities are abbreviated as follows: s = singlet, d = doublet, t = triplet, q = quartette, m = multiplet, br = broad;



Scheme 2. Synthesis of unsymmetrically (hetero)aromatic amine-substituted sulfamides **2r-w**.

Table 1. Calculated physicochemical properties and hCA I, II, IX and XII inhibitory profile of compounds **2a-w**.

Compound	Mw	cLogP ^d	Ki (nM) ^b			
			hCA I	hCA II	hCA IX	hCA XII
2a	180.2	-1.87	75.6	42.7	54.2	25.3
2b	179.2	-1.01	64.2	32.1	58.6	52.5
2c	204.2	0.42	126.2	70.5	30.7	51.7
2d	226.3	1.22	120.7	42.6	36.8	59.7
2e	180.2	-0.77	38.4	63.4	92.7	98.0
2f	208.2	-0.65	52.1	69.8	78.2	83.6
2g	193.3	-0.72	89.7	52.1	63.2	38.4
2h	240.3	1.57	359.5	120.4	58.2	96.7
2i	257.4	0.53	28.4	39.8	65.1	19.7
2j	187.2	-0.98	98.5	90.2	29.5	16.5
2k	192.3	0.15	22.6	48.2	73.2	66.8
2l	209.3	-0.12	59.6	92.3	126.5	72.5
2m	236.3	0.11	62.8	42.8	58.1	25.9
2n	247.4	0.43	497.3	99.3	72.5	35.1
2o	166.2	-1.05	59.2	66.9	82.1	100.9
2p	207.3	-1.39	88.2	59.4	46.2	40.2
2q	165.2	-1.60	68.9	52.9	78.2	100.2
2r	212.3	1.12	867.9	315.7	94.7	116.2
2s	174.2	-1.27	29.6	59.4	68.0	39.3
2t	212.3	1.31	231.4	89.5	34.2	114.2
2u	222.3	1.71	160.1	56.7	25.4	72.3
2v	198.2	0.79	723.5	472.2	102.5	95.7
2w	208.2	0.81	45.7	76.3	38.5	224.0
Acetazolamide			250	125	25	5.7

^aCalculated using Molinspiration Cheminformatics [34].

^bMean from three different assays, by a stopped flow technique (errors were in the range of ± 5 –10% of the reported values).

coupling constants, J , are reported in Hz. Mass spectra were recorded on a Bruker microTOF spectrometer (ESI ionization).

3.1.1. General procedure for the synthesis of compounds **2a-q**

A mixture of corresponding amine (2 mmol) and sulphuric diamide (8 mmol, 768 mg) in dry 1,4-dioxane (4 mL) was stirred at 110 °C for 48 h. If amine was in the form of hydrochloride salt, an additional equivalent of triethylamine was added. CH₂Cl₂ (5 mL) was added and the resulting precipitate was filtered off, washed with ethyl acetate (5 mL). The filtrate and the washings were combined and solvent was evaporated under reduced pressure. The crude product was purified by column chromatography on silica gel using CH₂Cl₂:2-propanol 20:1–10:1 gradient as eluent (R_f values are given for solvent system indicated).

3.1.2. 4-Hydroxypiperidine-1-sulphonamide (**2a**)

$R_f = 0.30$ (EtOAc); ¹H NMR (400 MHz, DMSO-*d*₆) $\delta = 6.66$ (s, 2H), 4.69 (d, $J = 3.9$ Hz, 1H), 3.58 (dq, $J = 7.8, 4.0$ Hz, 1H), 3.22 (ddd, $J = 11.0, 6.5, 3.8$ Hz, 2H), 2.74 (ddd, $J = 12.0, 9.0, 3.3$ Hz, 2H), 1.77 (ddt, $J = 13.7, 7.2, 3.6$ Hz, 2H), 1.46 (dtd, $J = 12.5, 8.6, 3.7$ Hz, 2H) ppm; ¹³C NMR (101 MHz, DMSO-*d*₆, DEPT) $\delta = 65.049$ (C-OH), 43.80 and 33.47 (2 CH₂) ppm; HRMS (ESI) C₅H₁₁N₂O₃S⁺ m/z : [M - H]⁻ 179.0492 (calc 179.0485).

3.1.3. 4-Methylpiperazine-1-sulphonamide (**2b**)

$R_f = 0.61$ (MeOH); ¹H NMR (400 MHz, DMSO-*d*₆) $\delta = 6.76$ (s, 2H), 2.95 (t, $J = 4.9$ Hz, 4H), 2.38 (t, $J = 5.0$ Hz, 4H), 2.19 (s, 3H) ppm; ¹³C NMR (101 MHz, DMSO-*d*₆, DEPT) $\delta = 54.08$ (CH₂), 46.14 (CH₂), 45.89 (CH₃) ppm; HRMS (ESI) C₅H₁₂N₃O₂S⁺ m/z : [M - H]⁻ 178.0644 (calc 178.0645).

3.1.4. N-(4-Fluorobenzyl)sulfamide (**2c**)

¹H NMR (400 MHz, DMSO-*d*₆) $\delta = 7.39$ (dd, $J = 8.5, 5.7$ Hz, 2H), 7.15 (t, $J = 8.9$ Hz, 2H), 7.07 (t, $J = 6.5$ Hz, 1H), 6.63 (s, 2H), 4.07 (d, $J = 6.5$ Hz, 2H) ppm; ¹³C NMR (101 MHz, DMSO-*d*₆, DEPT) $\delta = 161.70$ (d, $J = 242.2$ Hz), 135.39 (d, $J = 2.9$ Hz), 130.05 (d, $J = 8.1$ Hz, CH), 115.29 (d, $J = 21.3$ Hz, CH), 45.77 (s, CH₂) ppm; ¹⁹F NMR (470 MHz, DMSO-*d*₆) $\delta = -116.15$ ppm; HRMS (ESI) C₇H₉FN₂NaO₂S⁺ m/z : [M + Na]⁺ 227.0272 (calc 227.0261).

3.1.5. N-(1,2,3,4-Tetrahydronaphthalen-1-yl)sulfamide (**2d**)

$R_f = 0.80$ (CH₂Cl₂-CH₃OH 4:1); ¹H NMR (400 MHz, DMSO-*d*₆) $\delta = 7.57$ –7.50 (m, 1H), 7.19–7.11 (m, 2H), 7.08–7.02 (m, 1H), 6.96 (d, $J = 8.9$ Hz, 1H), 6.65 (s, 2H), 4.39 (td, $J = 8.0, 5.2$ Hz, 1H), 2.79–2.57 (m, 2H), 2.11–2.00 (m, 1H), 1.96–1.80 (m, 2H), 1.74–1.60 (m, 1H) ppm; ¹³C NMR (101 MHz, DMSO-*d*₆, DEPT) $\delta = 138.15, 137.41, 129.43, 128.94, 127.07, 126.02, 51.32$ (CH), 30.89, 29.23 and 20.39 (3CH₂) ppm; HRMS (ESI) C₁₀H₁₄N₂NaO₂S⁺ m/z : [M + Na]⁺ 249.0671 (calc 249.0668).

3.1.6. N-((tetrahydrofuran-2-yl)methyl)sulfamide (**2e**)

$R_f = 0.59$ (DCM:*i*-PrOH = 9:1); ¹H NMR (400 MHz, CDCl₃) $\delta = 4.94$ (br. t, $J = 6.0$ Hz, 1H), 4.88 (br. s, 2H), 4.08 (ddt, $J = 10.5, 7.3, 3.4$ Hz, 1H), 3.88 (dt, $J = 8.3, 6.7$ Hz, 1H), 3.82–3.73 (m, 1H), 3.28 (ddd,

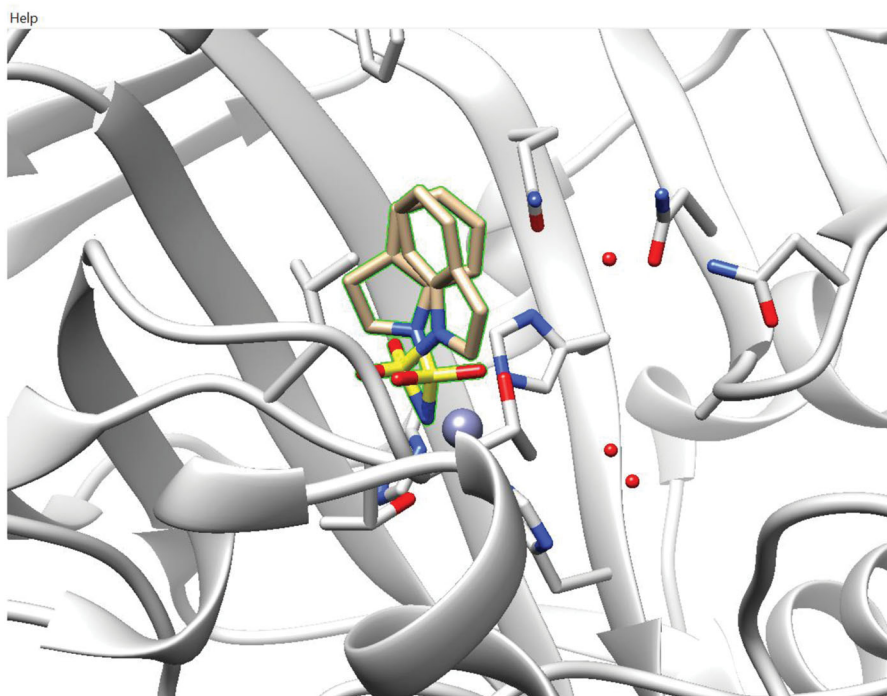


Figure 3. Co-crystal structure of fragment sulfamide 2v with hCA II (PDB code 7QSI).

$J = 13.3, 6.4, 3.2$ Hz, 1H), 3.14 (ddd, $J = 13.4, 7.8, 5.8$ Hz, 1H), 2.05 – 1.85 (m, 3H), 1.68 – 1.58 (m, 1H) ppm; ^{13}C NMR (101 MHz, CDCl_3 , DEPT) $\delta = 77.65$ (CH), 68.21, 47.52, 28.61 and 25.76 (4 CH_2) ppm; HRMS (ESI) $\text{C}_5\text{H}_{12}\text{N}_2\text{NaO}_3\text{S}^+$ m/z : $[\text{M} + \text{Na}]^+$ 203.0464 (calc 203.0461).

3.1.7. Methyl sulfamoylprolinate (2f)

$R_f = 0.75$ (EtOAc); ^1H NMR (400 MHz, $\text{DMSO-}d_6$) = 6.82 (s, 2H), 4.18 (dd, $J = 8.9, 4.1$ Hz, 1H), 3.27 (dq, $J = 6.2, 3.5, 2.9$ Hz, 2H), 2.18 – 2.07 (m, 1H), 1.92 – 1.80 (m, 3H) ppm; ^{13}C NMR (101 MHz, $\text{DMSO-}d_6$, DEPT) $\delta = 173.24, 60.47$ and 52.28 (CH and CH_3), 49.11, 31.06 and 24.92 (3 CH_2) ppm; HRMS (ESI) $\text{C}_6\text{H}_{13}\text{N}_2\text{O}_4\text{S}^+$ m/z : $[\text{M} + \text{H}]^+$ 209.0599 (calc 209.0591).

3.1.8. (1-Methylpiperidin-4-yl)sulfamide (2g)

$R_f = 0.13$ (MeOH); ^1H NMR (400 MHz, $\text{DMSO-}d_6$) $\delta = 6.47$ (s, 3H), 3.01 (tt, $J = 10.6, 4.2$ Hz, 1H), 2.68 (d, $J = 11.9$ Hz, 2H), 2.12 (s, 3H), 1.85 (qd, 11.9, 2.0 Hz, 4H), 1.42 (qd, $J = 12.5, 4.2$ Hz, 2H) ppm; ^{13}C NMR (101 MHz, $\text{DMSO-}d_6$) $\delta = 54.78, 50.36, 46.41, 32.86$ ppm; HRMS (ESI) $\text{C}_6\text{H}_{16}\text{N}_3\text{O}_2\text{S}^+$ m/z : $[\text{M} + \text{H}]^+$ 194.0955 (calc 194.0958).

3.1.9. 4-Phenylpiperidine-1-sulphonamide (2h)

$R_f = 0.86$ (EtOAc); ^1H NMR (400 MHz, $\text{DMSO-}d_6$) $\delta = 7.34 - 7.25$ (m, 4H), 7.21 (td, $J = 6.8, 1.7$ Hz, 1H), 6.75 (br.s, 2H), 3.59 (br.d, $J = 12.1$ Hz, 2H), 2.63 (td, $J = 12.2, 2.7$ Hz, 2H), 2.59 – 2.53 (m, 1H), 1.86 (br.d, $J = 12.2$ Hz, 2H), 1.69 (qd, $J = 12.5, 4.0$ Hz, 2H) ppm; ^{13}C NMR (101 MHz, $\text{DMSO-}d_6$, DEPT) $\delta = 145.97, 128.84$ ($\text{C}_{\text{Ar}}\text{H}$), 127.20 ($\text{C}_{\text{Ar}}\text{H}$), 126.67 ($\text{C}_{\text{Ar}}\text{H}$), 46.96 (CH_2), 41.45 (CH), 32.45 (CH_2) ppm; HRMS (ESI) $\text{C}_{11}\text{H}_{16}\text{N}_2\text{NaO}_2\text{S}^+$ m/z : $[\text{M} + \text{Na}]^+$ 263.0830 (calc 263.0825).

3.1.10. Benzyl (2-(dimethylamino)ethyl)sulfamide (2i)

$R_f = 0.58$ (MeOH); ^1H NMR (400 MHz, $\text{DMSO-}d_6$) $\delta = 7.40 - 7.33$ (m, 4H), 7.31 – 7.26 (m, 1H), 6.91 (s, 2H), 4.26 (s, 2H), 3.09 (t, $J = 6.8$ Hz, 2H), 2.30 (t, $J = 6.8$ Hz, 2H), 2.07 (s, 6H) ppm; ^{13}C NMR (101 MHz, $\text{DMSO-}d_6$, DEPT) $\delta = 138.06, 128.76, 128.56$ and 127.74 (3 $\text{C}_{\text{Ar}}\text{H}$), 57.05, 51.41 and 45.72 (3 CH_2), 45.52 (CH_3) ppm; HRMS (ESI) $\text{C}_{11}\text{H}_{20}\text{N}_3\text{O}_2\text{S}^+$ m/z : $[\text{M} + \text{H}]^+$ 258.1276 (calc 258.1271).

3.1.11. (Pyridin-3-ylmethyl)sulfamide (2j)

$R_f = 0.90$ (MeOH); ^1H NMR (400 MHz, CD_3CN) $\delta = 8.55$ (d, $J = 2.2$ Hz, 1H), 8.48 (dd, $J = 4.8, 1.6$ Hz, 1H), 7.76 (dt, $J = 7.9, 1.9$ Hz, 1H), 7.33 (dd, $J = 7.8, 4.8$ Hz, 1H), 5.62 (br. s, 1H), 5.31 (br. s, 2H), 4.20 (d, $J = 6.3$ Hz, 2H) ppm; ^{13}C NMR (101 MHz, CD_3CN) $\delta = 149.23, 148.59, 135.72, 133.71, 123.46, 44.32$ ppm; HRMS (ESI) $\text{C}_6\text{H}_9\text{N}_3\text{NaO}_2\text{S}^+$ m/z : $[\text{M} + \text{Na}]^+$ 210.0308 (calc 210.0308).

3.1.12. (Thiophen-2-ylmethyl) sulfamide (2k)

$R_f = 0.49$ (DCM:*i*-PrOH = 20:1); ^1H NMR (400 MHz, Acetone- d_6) = 7.37 (dd, $J = 5.2, 1.2$ Hz, 1H), 7.07 (dq, $J = 3.3, 1.1$ Hz, 1H), 6.97 (dd, $J = 5.1, 3.5$ Hz, 1H), 6.20 (s, 1H), 5.99 (s, 2H), 4.45 (dd, $J = 6.4, 1.0$ Hz, 2H) ppm; ^{13}C NMR (101 MHz, Acetone- d_6 , DEPT) $\delta = 141.21$ ($>\text{C}=\text{}$), 126.62, 125.80, and 125.08 (3 $\text{C}_{\text{Ar}}\text{H}$), 41.97 (CH_2) ppm; HRMS (ESI) $\text{C}_5\text{H}_8\text{N}_2\text{NaO}_2\text{S}_2^+$ m/z : $[\text{M} + \text{Na}]^+$ 214.9919 and 216.9877 (calc 214.9919 and 216.9878).

3.1.13. (2-(Diethylamino)ethyl)(methyl)sulfamide (2l)

$R_f = 0.58$ (MeOH); ^1H NMR (400 MHz, $\text{DMSO-}d_6$) = 6.73 (s, 2H), 3.05 (t, $J = 6.8$ Hz, 2H), 2.68 (s, 2H), 2.55 (t, $J = 6.8$ Hz, 2H), 2.49 (q, $J = 7.1$ Hz, 4H), 0.96 (t, $J = 7.1$ Hz, 6H) ppm; ^{13}C NMR (101 MHz, $\text{DMSO-}d_6$, DEPT) $\delta = 50.53, 48.57$ and 46.95 (3 CH_2), 35.57 and 12.01 (2 CH_3) ppm; HRMS (ESI) $\text{C}_7\text{H}_{20}\text{N}_3\text{O}_2\text{S}^+$ m/z : $[\text{M} + \text{H}]^+$ 210.1274 (calc 210.1271).

3.1.14. Ethyl 1-sulfamoylpiperidine-4-carboxylate (2m)

$R_f = 0.81$ (EtOAc); $^1\text{H NMR}$ (400 MHz, DMSO- d_6) $\delta = 6.71$ (s, 2H), 4.07 (q, $J = 7.1$ Hz, 2H), 3.36 (dt, $J = 12.3, 3.8$ Hz, 2H), 2.62 (td, $J = 11.6, 2.8$ Hz, 2H), 2.42 (tt, $J = 10.7, 4.0$ Hz, 1H), 1.90 (br. dd, $J = 13.5, 3.8$ Hz, 2H), 1.60 (qd, $J = 11.1, 3.8$ Hz, 2H), 1.18 (t, $J = 7.1$ Hz, 3H) ppm; $^{13}\text{C NMR}$ (101 MHz, DMSO- d_6) $\delta = 174.25, 60.44, 45.55, 27.47, 14.54$ ppm; HRMS (ESI) $\text{C}_8\text{H}_{16}\text{N}_2\text{NaO}_4\text{S}^+$ m/z : $[\text{M} + \text{Na}]^+ 259.0722$ (calc 259.0723).

3.1.15. [1,4'-Bipiperidine]-1'-sulphonamide (2n)

$R_f = 0.24$ (MeOH); $^1\text{H NMR}$ (400 MHz, DMSO- d_6) $\delta = 6.68$ (br.s, 2H), 3.48 (br.d, $J = 12.4$ Hz, 2H), 2.53–2.41 (m, 3H), 2.44 (t, $J = 5.1$ Hz, 3H), 2.24 (tt, $J = 11.3, 3.6$ Hz, 1H), 1.76 (br.d, $J = 11.7$ Hz, 2H), 1.52–1.43 (m, 6H), 1.38 (q, $J = 5.9$ Hz, 2H) ppm; $^{13}\text{C NMR}$ (101 MHz, DMSO- d_6 , DEPT) $\delta = 61.56, 50.16, 46.22, 27.21, 26.52, 25.01$; HRMS (ESI) $\text{C}_{10}\text{H}_{22}\text{N}_3\text{O}_2\text{S}^+$ m/z : $[\text{M} + \text{H}]^+ 248.1431$ (calc 248.1428).

3.1.16. Morpholine-4-sulphonamide (2o)

$R_f = 0.56$ (EtOAc); $^1\text{H NMR}$ (400 MHz, DMSO- d_6) $\delta = 6.82$ (s, 2H), 3.86–3.50 (m, 4H), 3.02–2.77 (m, 4H) ppm; $^{13}\text{C NMR}$ (101 MHz, DMSO- d_6) $\delta = 65.73, 46.43$ ppm; HRMS (ESI) $\text{C}_4\text{H}_9\text{N}_2\text{O}_3\text{S}^+$ m/z : $[\text{M} - \text{H}]^- 165.0326$ (calc 165.0339)

3.1.17. 1-Sulfamoylpiperidine-4-carboxamide (2p)

$R_f = 0.61$ (EtOAc:MeOH 3:1); $^1\text{H NMR}$ (400 MHz, DMSO- d_6) $\delta = 7.27$ (s, 1H), 6.82 (s, 1H), 6.79–6.44 (m, 2H), 3.52–3.39 (m, 2H), 2.21–2.05 (m, 1H), 1.78 (d, $J = 13.1$ Hz, 2H), 1.57 (t, $J = 12.7$ Hz, 2H) ppm; $^{13}\text{C NMR}$ (101 MHz, DMSO- d_6) $\delta = 176.30, 45.96, 41.12, 28.07$ ppm; HRMS (ESI) $\text{C}_6\text{H}_{13}\text{N}_3\text{NaO}_3\text{S}^+$ m/z : $[\text{M} + \text{Na}]^+ 230.0565$ (calc 230.0570)

3.1.18. Piperazine-1-sulphonamide hydrochloride (2q)

$^1\text{H NMR}$ (400 MHz, DMSO- d_6) $\delta = 9.60$ (s, 2H), 7.08 (s, 2H), 3.21 (dd, $J = 7.1, 3.6$ Hz, 4H), 3.14 (dd, $J = 7.0, 3.7$ Hz, 4H) ppm; $^{13}\text{C NMR}$ (101 MHz, DMSO- d_6) $\delta = 43.27, 42.37$ ppm; HRMS (ESI) $\text{C}_4\text{H}_{12}\text{N}_3\text{O}_2\text{S}^+$ m/z : $[\text{M} + \text{H}]^- 166.0649$ (calc 166.0645).

3.1.19. 2-Methylindoline-1-sulphonamide (2r)

$R_f = 0.81$ (n-Hexane:EtOAc 1:1); $^1\text{H NMR}$ (400 MHz, CDCl_3) $\delta = 7.40$ (d, $J = 8.2$ Hz, 1H), 7.19 (dt, $J = 7.7, 3.7$ Hz, 2H), 7.04 (t, $J = 7.4$ Hz, 1H), 4.46 (s br., 1H), 4.07 (s br., 2H), 3.52–3.43 (m, 2H), 2.67 (dd, $J = 15.9, 3.5$ Hz, 1H), 1.43 (d, $J = 6.1$ Hz, 3H) ppm; $^{13}\text{C NMR}$ (101 MHz, CDCl_3) $\delta = 141.32, 131.15, 127.79, 125.40, 124.10, 115.77, 59.19, 36.64, 22.63$ ppm; HRMS (ESI) $\text{C}_9\text{H}_{12}\text{N}_2\text{NaO}_2\text{S}^+$ m/z : $[\text{M} + \text{Na}]^+ 235.0515$ (calc 235.0512).

3.1.20. N-(Pyrimidin-2-yl)sulfamide (2s)

$^1\text{H NMR}$ (400 MHz, DMSO- d_6) $\delta = 8.56$ (d, $J = 4.8$ Hz, 4H), 7.06 (t, $J = 4.9$ Hz, 2H) ppm; $^{13}\text{C NMR}$ (101 MHz, DMSO- d_6) $\delta = 158.73, 158.26, 115.28$ ppm; HRMS (ESI) $\text{C}_4\text{H}_6\text{N}_4\text{NaO}_2\text{S}^+$ m/z : $[\text{M} + \text{Na}]^+ 197.1668$ (calc 197.1672)

3.1.21. 3,4-Dihydroquinoline-1(2H)-sulphonamide (2t)

$R_f = 0.55$ (n-Hexane:EtOAc 3:1); $^1\text{H NMR}$ (400 MHz, CDCl_3) $\delta = 7.67$ (d, $J = 8.2$ Hz, 1H), 7.17 (t, $J = 7.6$ Hz, 1H), 7.14–7.02 (m, 2H), 4.56 (s, 2H), 3.87–3.53 (m, 2H), 2.86 (t, $J = 6.6$ Hz, 2H), 2.06 (p,

$J = 6.5$ Hz, 2H) ppm; $^{13}\text{C NMR}$ (400 MHz, CDCl_3 , DEPT) $\delta = 137.20, 129.92, 129.53, 126.60, 124.65$ and 123.61 (4 $\text{C}_{\text{Ar}}\text{H}$), 47.28, 26.94 and 21.87 (3 CH_2) ppm; HRMS (ESI) $\text{C}_9\text{H}_{12}\text{N}_2\text{NaO}_2\text{S}^+$ m/z : $[\text{M} + \text{Na}]^+ 235.05110$ (calc 235.0511)

3.1.22. N-(Naphthalen-1-yl)sulfamide (2u)

$R_f = 0.44$ (n-Hexane:EtOAc 1:1); $^1\text{H NMR}$ (400 MHz, DMSO- d_6) $\delta = 9.27$ (s, 1H), 8.35–8.25 (m, 1H), 7.96–7.87 (m, 1H), 7.75 (d, $J = 8.1$ Hz, 1H), 7.59 (dd, $J = 7.6, 1.2$ Hz, 1H), 7.55–7.47 (m, 3H), 7.00 (s, 2H) ppm; $^{13}\text{C NMR}$ (101 MHz, DMSO- d_6 , DEPT) $\delta = 134.74, 134.36, 129.17, 128.26, 126.43, 126.10, 125.49, 124.10, 121.57$ ppm; HRMS (ESI) $\text{C}_{10}\text{H}_{10}\text{N}_2\text{NaO}_2\text{S}^+$ m/z : $[\text{M} + \text{Na}]^+ 245.0359$ (calc 245.0356)

3.1.23. Indoline-1-sulphonamide (2v)

$R_f = 0.77$ (EtOAc); $^1\text{H NMR}$ (400 MHz, DMSO- d_6) $\delta = 7.28$ (d, $J = 8.0$ Hz, 1H), 7.25–7.20 (m, 1H), 7.23 (s, 2H), 7.16 (t, $J = 7.7$ Hz, 1H), 6.96 (t, $J = 7.4$ Hz, 1H), 3.80 (t, $J = 8.4$ Hz, 2H), 3.05 (t, $J = 8.4$ Hz, 2H) ppm; $^{13}\text{C NMR}$ (101 MHz, DMSO- d_6 , DEPT) $\delta = 143.51$ and 131.99 (2 $>\text{C}_{\text{Ar}}\text{=}$), 127.63, 125.40, 122.83 and 114.21 (4 $\text{C}_{\text{Ar}}\text{H}$), 50.39 (CH_2), 27.76 (CH_2) ppm; HRMS (ESI) $\text{C}_8\text{H}_{10}\text{N}_2\text{NaO}_2\text{S}^+$ m/z : $[\text{M} + \text{Na}]^+ 221.0357$ (calc 221.0355)

3.1.24. N-(2,4-Difluorophenyl)sulfamide (2w)

$^1\text{H NMR}$ (400 MHz, CDCl_3) $\delta = 7.40$ (d, $J = 8.2$ Hz, 1H), 7.19 (dt, $J = 7.7, 3.7$ Hz, 2H), 7.04 (t, $J = 7.4$ Hz, 1H), 4.46 (s br., 1H), 4.07 (s br., 2H), 3.52–3.43 (m, 2H), 2.67 (dd, $J = 15.9, 3.5$ Hz, 1H), 1.43 (d, $J = 6.1$ Hz, 3H) ppm; $^{13}\text{C NMR}$ (101 MHz, CDCl_3) $\delta = 160.29$ (dd, $J = 248.7, 11.3$ Hz), 154.88 (dd, $J = 247.7, 12.1$ Hz), 125.60 (dd, $J = 9.6, 1.4$ Hz, $\text{C}_{\text{Ar}}\text{H}$), 121.02 (dd, $J = 12.5, 3.7$ Hz), 111.97 (dd, $J = 22.3, 3.8$ Hz), 104.40 (dd, $J = 26.7, 23.7$ Hz) ppm; $^{19}\text{F NMR}$ (376 MHz, CDCl_3) $\delta = -111.98, -123.53$ ppm; HRMS (ESI) $\text{C}_6\text{H}_6\text{F}_2\text{N}_2\text{NaO}_2\text{S}^+$ m/z : $[\text{M} + \text{Na}]^+ 231.0010$ (calc 231.0011)

3.2. Carbonic anhydrase inhibition testing

An Applied Photophysics stopped-flow instrument has been used for assaying the CA catalysed CO_2 hydration activity³⁵. Phenol red (at a concentration of 0.2 mM) has been used as indicator, working at the absorbance maximum of 557 nm, with 20 mM Hepes (pH 7.5) as buffer, and 20 mM Na_2SO_4 (for maintaining constant the ionic strength), following the initial rates of the CA-catalysed CO_2 hydration reaction for a period of 10–100 s. The CO_2 concentrations ranged from 1.7 to 17 mM for the determination of the kinetic parameters and inhibition constants. For each inhibitor at least six traces of the initial 5–10% of the reaction have been used for determining the initial velocity. The uncatalyzed rates were determined in the same manner and subtracted from the total observed rates. Stock solutions of inhibitor (0.1 mM) were prepared in distilled deionised water and dilutions up to 0.01 nM were done thereafter with the assay buffer. Inhibitor and enzyme solutions were preincubated together for 15 min at room temperature prior to assay, in order to allow for the formation of the EI complex. The inhibition constants were subsequently obtained by nonlinear least-squares methods using PRISM 3 and the ChengPrusoff equation, as reported earlier, and represent the mean from at least three different determinations. All CA isoforms were recombinant ones obtained in-house as reported earlier^{36–39}.

Table 2. Summary of data collection and atomic model refinement statistics for *hCAII*.^a

	<i>hCAII</i> + 2v
PDB ID	7QSI
Wavelength (Å)	0.999900
Space Group	P21
Unit cell (a, b, c, α , β , γ) (Å,°)	42.363, 41.557, 72.068 90.000, 104.495, 90.000
Limiting resolution (Å)	41.02–1.30 (1.34–1.30)
Unique reflections	52,866 (2056)
Rmerge (%)	6.4 (73.2)
Rmeas (%)	7.0 (84.4)
Redundancy	6.11 (3.98)
Completeness overall (%)	88.9 (46.7)
$\langle I/\sigma(I) \rangle$	19.54 (2.1)
CC (1/2)	99.9 (63.8)
Refinement statistics	
Resolution range (Å)	41.02–1.30
Rfactor (%)	16.27
Rfree(%)	18.45
r.m.s.d. bonds(Å)	0.0135
r.m.s.d. angles (°)	1.8542
Ramachandran statistics (%)	
Most favoured	96.9
additionally allowed	3.1
outlier regions	0.0
Average B factor (Å ²)	
All atoms	15.116
inhibitors	11.348
Solvent	24.123

^aValues in parentheses are for the highest resolution shell.

3.3. Co-crystallization and X-ray data collection

Crystals of *hCA II* complexed with compound **2v** were obtained using the sitting drop vapour diffusion method. An equal volume of 0.8 mM solution of *hCA II* in Tris pH = 8.0 and 1.6 mM of the inhibitors in Hepes 20 mM pH = 7.4 was mixed and incubated for 15 min. 2 mL of the complex solution were mixed with 2 mL of a solution of 1.6 M sodium citrate, 50 mM Tris pH 8.0 and were equilibrated against the same solution at 296 K. Crystals of the complex grew in a few days. The crystals were flash-frozen at 100 K using a solution obtained by adding 25% (v/v) glycerol to the mother liquor solution as cryoprotectant. A data set on a crystal of the complex with the inhibitor **2v** was collected at the Centro di Cristallografia Strutturale (CRIST) in Florence using an Oxford Diffraction instrument equipped with a sealed tube Enhance Ultra (Cu) and a Onyx CCD detector. Data were integrated and scaled using the program XDS.24 Data processing statistics are showed in Table 2.

3.4. Structure determination

The crystal structure of *hCA II* (PDB accession code: 7QSI) without solvent molecules and other heteroatoms was used to obtain initial phases of the structures using Refmac5⁴⁰. 5% of the unique reflections were selected randomly and excluded from the refinement data set for the purpose of Rfree calculations. The initial |Fo-Fc| difference electron density maps unambiguously showed the inhibitor molecules. An electron density, which could be interpreted as a second molecule of inhibitor **2v**, was present near the N-terminus of the protein. Thus, a second **2v** molecule was introduced in the model with 0.75 occupancy. Atomic model for the inhibitor was calculated and energy minimised using the program JLigand 1.0.39. Refinements proceeded using normal protocols of positional, isotropic atomic displacement parameters alternating with manual building of the models using COOT⁴¹. Solvent molecules were introduced automatically using the program ARP⁴². The quality of the final model was assessed with COOT and

Rampage⁴³. Crystal parameters and refinement data are summarised in Table 2. Atomic coordinates were deposited in the Protein Data Bank (PDB accession code: 7QSI). Graphical representations were generated with Chimera⁴⁴.

4. Conclusions

We have described the synthesis and testing against a panel of human carbonic anhydrases (*hCA I, II, IX and XII*) of a series of hydrophilic, fragment sulfamides intended for fragment-based drug discovery of isoform-selective carbonic anhydrase inhibitors via cooperative screening with other, non-zinc-binding fragments. As expected from the minimal-periphery zinc-binding moieties, these fragment sulfamides demonstrated little selectivity across the panel of *hCAs*. However, for one of the fragment inhibitors (**2v**) which showed higher selectivity towards the cancer-related *hCA* isoforms (*IX and CII*), we obtained a crystal structure with the most abundant cytosolic isoform *hCA II* which showed two possible binding modes and thus significant room for cooperative fragment binding and subsequent periphery evolution.

Supplementary materials

Copies of ¹H and ¹³C NMR spectra of compounds **2a–w**.

Acknowledgements

We are grateful to the Research Centre for Magnetic Resonance and the Centre for Chemical Analysis and Materials Research of Saint Petersburg State University Research Park for the analytical data.

Disclosure statement

No potential conflict of interest was reported by all author(s) except CTS. CT Supuran is Editor-in-Chief of the Journal of Enzyme Inhibition and Medicinal Chemistry. He was not involved in the assessment, peer review, or decision-making process of this paper. The authors have no relevant affiliations of financial involvement with any organisation or entity with a financial interest in or financial conflict with the subject matter or materials discussed in the manuscript. This includes employment, consultancies, honoraria, stock ownership or options, expert testimony, grants or patents received or pending, or royalties. This article was submitted before the start of the Russia-Ukraine military conflict on February 24, 2022.

Funding

This research was supported by the Ministry of Education of the Russian Federation [government contract 073-00077-21-02 "Development of an innovative glaucoma drug based on selective inhibition of carbonic anhydrase II," registry number 730000Φ.99.1.ББ10АА00006].

ORCID

Alessio Nocentini  <http://orcid.org/0000-0003-3342-702X>
 Andrea Angeli  <http://orcid.org/0000-0002-1470-7192>
 Claudiu T. Supuran  <http://orcid.org/0000-0003-4262-0323>

References

- Pastorekova S, Parkkila S, Pastorek J, Supuran CT. Carbonic anhydrases: current state of the art, therapeutic applications and future prospects. *J Enzyme Inhib Med Chem* 2004;19:199–229.
- Alterio V, Di Fiore A, D'Ambrosio K, et al. Multiple binding modes of inhibitors to carbonic anhydrases: how to design specific drugs targeting 15 different isoforms? *Chem Rev* 2012;112:4421–68.
- Supuran CT. Structure-based drug discovery of carbonic anhydrase inhibitors. *J Enzyme Inhib Med Chem* 2012;27:759–72.
- Scozzafava A, Supuran CT. Glaucoma and the applications of carbonic anhydrase inhibitors. *Subcell Biochem* 2014;75:349–59.
- Supuran CT. Acetazolamide for the treatment of idiopathic intracranial hypertension. *Expert Rev Neurother* 2015;15:851–6.
- Swenson ER. Carbonic anhydrase inhibitors and high altitude illnesses. *Subcell Biochem* 2014;75:361–86.
- Wongboonsin J, Thongprayoon C, Bathini T, et al. Acetazolamide therapy in patients with heart failure: a meta-analysis. *J Clin Med* 2019;8:349.
- Buzás GM, Supuran CT. The history and rationale of using carbonic anhydrase inhibitors in the treatment of peptic ulcers. In memoriam Ioan Pușcaș (1932–2015). *J Enzyme Inhib Med Chem* 2016;31:527–33.
- Ciccione L, Cerri C, Nencetti S, Orlandini E. Carbonic anhydrase and epilepsy: state of the art and future perspectives. *Molecules* 2021;26:6380.
- Mboge MY, McKenna R, Frost SC. Advances in anti-cancer drug development targeting carbonic anhydrase IX and XII. *Top Anticancer Res* 2015;5:3–42.
- Ward C, Meehan J, Gray ME, et al. The impact of tumour pH on cancer progression: strategies for clinical intervention. *Explor Target Antitumor Ther* 2020;1:71–100.
- Carta F, Vullo D, Osman SM, et al. Synthesis and carbonic anhydrase inhibition of a series of SLC-0111 analogs. *Bioorg Med Chem* 2017;25:2569–76.
- <https://clinicaltrials.gov/ct2/show/NCT03450018> [last accessed 14 Jan 2022].
- Assi R, Kantarjian H, Kadia TM, et al. Final results of a phase 2, open-label study of Indisulam, idarubicin, and cytarabine in patients with relapsed or refractory acute myeloid leukemia and high-risk myelodysplastic syndrome. *Cancer* 2018;124:2758–65.
- Supuran CT, Capasso C. Antibacterial carbonic anhydrase inhibitors: an update on the recent literature. *Exp Opin Ther Pat* 2020;30:963–82.
- De Vita D, Angeli A, Pandofi F, et al. Inhibition of the α -carbonic anhydrase from *Vibrio cholerae* with amides and sulfonamides incorporating imidazole moieties. *J Enzyme Inhib Med Chem* 2017;32:798–804.
- Rasti B, Mazraedoost S, Panahi H, et al. New insights into the selective inhibition of the β -carbonic anhydrases of pathogenic bacteria *Burkholderia pseudomallei* and *Francisella tularensis*: a proteochemometrics study. *Mol Divers* 2019;23:263–73.
- Aspatwar A, Winum J-Y, Carta F, et al. Carbonic anhydrase inhibitors as novel drugs against mycobacterial β -carbonic anhydrases: an update on in vitro and in vivo studies. *Molecules* 2018;23:2911.
- Nishimori I, Minakuchi T, Vullo D, et al. Inhibition studies of the β -carbonic anhydrases from the bacterial pathogen *Salmonella enterica* serovar Typhimurium with sulfonamides and sulfamates. *Bioorg Med Chem* 2011;19:5023–30.
- Grande R, Carradori S, Puca V, et al. Selective inhibition of *Helicobacter pylori* carbonic anhydrases by carvacrol and thymol could impair biofilm production and the release of outer membrane vesicles. *Int J Mol Sci* 2021;22:11583.
- Del Prete S, De Luca V, Bua S, et al. The effect of substituted benzene-sulfonamides and clinically licensed drugs on the catalytic activity of CynT2, a carbonic anhydrase crucial for *Escherichia coli* life cycle. *Int J Mol Sci* 2020;21:4175.
- Winum J-Y, Scozzafava A, Montero J-L, Supuran CT. New zinc binding motifs in the design of selective carbonic anhydrase inhibitors. *Mini-Rev Med Chem* 2006;6:921–36.
- Yue EW, Sparks R, Polam P, et al. INCB24360 (Epcadostat), a highly potent and selective indoleamine-2,3-dioxygenase 1 (IDO1) inhibitor for immuno-oncology. *ACS Med Chem Lett* 2017;8:486–91.
- Langtry HD, Grant SM, Goa KL. Famotidine. An updated review of its pharmacodynamic and pharmacokinetic properties, and therapeutic use in peptic ulcer disease and other allied diseases. *Drugs* 1989;38:551–90.
- Angeli A, Ferraroni M, Nocentini A, et al. Polypharmacology of epcadostat: a potent and selective inhibitor of the tumor associated carbonic anhydrases IX and XII. *Chem Commun (Camb)* 2019;55:5720–3.
- Angeli A, Ferraroni M, Supuran CT. Famotidine, an antiulcer agent, strongly inhibits *Helicobacter pylori* and human carbonic anhydrases. *ACS Med Chem Lett* 2018;9:1035–8.
- Krasavin M, Kalinin S, Zozulya S, et al. Screening of benzene-sulfonamide in combination with chemically diverse fragments against carbonic anhydrase by differential scanning fluorimetry. *J Enzyme Inhib Med Chem* 2020;35:306–10.
- Li Q. Application of fragment-based drug discovery to versatile targets. *Front Mol Biosci* 2020;7:180.
- According to the Reaxys database, only 9,106 sulfamides (NSO₂NH₂) were associated with the keywords “carbonic anhydrase inhibitor” compared to 108,988 sulfonamides searchable in the same context (information retrieved on January 18, 2022).
- Bonardi A, Nocentini A, Bua S, et al. Sulfonamide inhibitors of human carbonic anhydrases designed through a three-tails approach: improving ligand/isoform matching and selectivity of action. *J Med Chem* 2020;63:7422–44.
- Ferreira LG, Andricopulo AD. From protein structure to small-molecules: recent advances and applications to fragment-based drug discovery. *Curr Top Med Chem* 2017;17:2260–70.
- Xu Z, Tice CM, Zhao W, et al. Structure-based design and synthesis of 1,3-oxazinan-2-one inhibitors of 11 β -hydroxysteroid dehydrogenase type 1. *J Med Chem* 2011;54:6050–62.
- Casini A, Winum J-Y, Montero J-L, et al. Carbonic anhydrase inhibitors: inhibition of cytosolic isozymes I and II with sulfamide derivatives. *Bioorg. Med. Chem. Lett* 2003;13:837–40.
- <https://www.molinspiration.com/>.
- Khalifah RG. The carbon dioxide hydration activity of carbonic anhydrase. I. Stop-flow kinetic studies on the native human isoenzymes B and C. *J Biol Chem* 1971;246:2561–73.
- Wilkinson BL, Bornaghi LF, Houston TA, et al. A novel class of carbonic anhydrase inhibitors: glycoconjugate benzene sulfonamides prepared by “click-tailing”. *J Med Chem* 2006;49:6539–48.

37. Lopez M, Salmon AJ, Supuran CT, Poulsen S-A. Carbonic anhydrase inhibitors developed through 'click tailing'. *Curr Pharm Des* 2010;16:3277-87.
38. Wilkinson BL, Bornaghi LF, Houston TA, et al. Carbonic anhydrase inhibitors: inhibition of isozymes I, II, and IX with triazole-linked O-glycosides of benzene sulfonamides. *J Med Chem* 2007;50:1651-7.
39. Pala N, Micheletto L, Sechi M, et al. Carbonic anhydrase inhibition with benzenesulfonamides and tetrafluorobenzenesulfonamides obtained via click chemistry. *ACS Med Chem Lett* 2014;5:927-30.
40. Murshudov GN, Vagin AA, Dodson EJ. Refinement of macromolecular structures by the maximum-likelihood method. *Acta Crystallogr D Biol Crystallogr* 1997; 53:240-55.
41. Emsley P, Lohkamp B, Scott W, Cowtan K. Features and development of Coot. *Acta Crystallogr D Biol Crystallogr* 2010;66:486-501.
42. Lamzin VS, Perrakis A, Wilson KS. The ARP/WARP suite for automated construction and refinement of protein models. In: Rossmann MG, Arnold E, eds. *Int. Tables for crystallography*. Vol. F: Crystallography of biological macromolecules. Dordrecht, The Netherlands: Kluwer Academic Publishers; 2001:720-722.
43. Lovell SC, Davis IW, Arendall WB, III, et al. Structure validation by $C\alpha$ geometry: ϕ, ψ and $C\beta$ deviation. *Proteins Struct Funct Genet* 2003;50:437-50.
44. Pettersen EF, Goddard TD, Huang CC, et al. UCSF Chimera-a visualization system for exploratory research and analysis. *J Comput Chem* 2004;25:1605-12.